ELSEVIER

Int. J. Therm. Sci. 41 (2002) 386–395

International Journal of Thermal Sciences

www.elsevier.com/locate/ijts

# Time-dependent heat transfer in a fin-wall assembly. New performance coefficient: thermal reverse admittance

Mariano Alarcón [a], Francisco Alhama [b], Carlos F. González-Fernández [b,*]

[a] Thermal Machines and Heat Engines Area, University of Murcia, 30100 Campus de Espinardo, Murcia, Spain
[b] Department of Applied Physics, Tech. University of Cartagena, Campus Muralla del Mar, 30203 Cartagena, Murcia, Spain

Received 19 August 2000; accepted 18 June 2001

**Abstract**

Transient thermal fields and heat fluxes due to step-harmonic temperature excitation and their dependence on frequency are studied in a fin-wall assembly. Application of the currently used efficiency coefficient to transient-harmonic processes is discussed. A new coefficient, thermal reverse transfer admittance, and others, including the augmentation factor, have been used to characterise the behaviour of the system. In a thermal frequency response analysis, module, phase, real and imaginary components have been obtained. For the calculation a network model (whose admittance is identical to the thermal admittance of the system) has been designed for the whole system. The network simulation method provides the numerical response of the system by running the network in circuit resolution software. © 2002 Éditions scientifiques et médicales Elsevier SAS. All rights reserved.

*Keywords:* Harmonic excitation; Transient heat conduction; Fins (heat exchange); Thermal reverse admittance; Network simulation method

## 1. Introduction

Different papers have been written by several authors that study the transient heat transfer in individual straight fins under harmonic boundary conditions; most of them do not take into account the effect of the supporting interface (wall). In this sense, Yang [1] analytically studied the pseudo-steady state response (i.e., the stationary-oscillating regime) of an isolated straight fin whose temperature at its base is harmonically changing. He determined that both the temperature and heat flux throughout the fin are characterised by a stationary value due to the steady-state boundary conditions and a transient value of the same frequency but different module and phase than that of the excitation. Aziz [2] made a similar study on annular fins. Suryanarayana [3,4] studied the transient behaviour of the straight fin under sinusoidal excitation, and considered a convective boundary condition at the base of the fin that is close to the actual fin-wall configuration. He did not take into account the wall thermal resistance and capacity. Other geometries such as annular fins, triangular profiles and 2-D configurations under harmonic excitation have also been studied by Chu et al., [5], Wu et al., [6], etc. Yang and He [7] dedicated a paper to the trapezoidal fin with thermal dependent conductivity. Papadopoulos et al. [8] have studied the transient problem for straight fins whose surrounding medium has temperature varying as a sinusoidal function.

Nevertheless, the isolated fin is merely an idealisation. One of the main aspects to consider in applications including a set of fins is the influence of the *primary surface* (wall). The influence of the wall to which the fin is attached is quite important for assembly performance. The study of the fin-wall system as a set is a far more realistic approach that also allows the consideration of fin arrays. The fin-wall assembly has been studied, both as 1-D and 2-D systems, by Suryanarayana [9], Heggs and Stones [10], Manzoor et al. [11,12], Huang and Shah [13], Jucá and Prata [14], Wood et al. [15], Thomas [16], etc. The latter concludes that when fin and wall are of the same material, the consideration of the fin-wall set makes the bidimensional effects negligible in practical applications.

* Correspondence and reprints.
*E-mail addresses:* mariano@um.es (M. Alarcón), paco.alhama@upct.es (F. Alhama), carlosf.gonzalez@upct.es (C.F. González-Fernández).

1290-0729/02/$ – see front matter © 2002 Éditions scientifiques et médicales Elsevier SAS. All rights reserved.
PII: S1290-0729(02)01329-7

**Nomenclature**

| | | |
|---|---|---|
| $A$ | dimensionless oscillation amplitude | |
| *Aug* | augmentation | |
| $b$ | width of the fin | m |
| $B$ | dimensionless angular speed $= \omega L_f^2/\alpha$ | |
| $Bi_1$ | modified Biot number $= hL_y^2/kL_w$ | |
| $c$ | specific heat | $kJ \cdot kg^{-1} \cdot K^{-1}$ |
| $C$ | heat capacity | $kJ \cdot m^{-2} \cdot K^{-1}$ |
| $e$ | half fin thickness | m, error % |
| $h$ | heat transfer coefficient | $W \cdot m^{-2} \cdot K^{-1}$ |
| $f$ | frequency | $s^{-1}$ |
| *Fo* | Fourier number $= t\alpha/L_f^2$ | |
| $j$ | heat rate density | $W \cdot m^{-2}$ |
| $J$ | heat rate | W |
| $k$ | thermal conductivity of the material | $W \cdot m^{-1} \cdot K^{-1}$ |
| $L$ | length | m |
| $M$ | dimensionless fin parameter $= (2h_{2f}L_f^2/2ek_f)^{1/2}$ | |
| $N$ | number of fin volume compartments or cells | |
| $P$ | perimeter of the fin | m |
| $R$ | thermal resistance | $K \cdot W^{-1}$ |
| $S$ | cross-sectional area | $m^2$ |
| $S_f^*$ | external fin area | $m^2$ |
| $t$ | time | s |
| $T$ | temperature of the material at point $x$ | K |
| $x, y$ | space co-ordinates | m |
| $Y$ | thermal (reverse or input) admittance | $W \cdot K^{-1}$ |

*Greek symbols*

| | | |
|---|---|---|
| $\alpha$ | thermal diffusivity | $m^2 \cdot s^{-1}$ |
| $\Delta\varphi$ | phase delay (rad or degrees) | |
| $\Delta x$ | length of each compartment | m |
| $\eta$ | efficiency | |
| $\varphi$ | phase (rad or degrees) | |
| $\rho$ | density | $kg \cdot m^{-3}$ |
| $\theta$ | temperature excess, i.e., temperature difference between point $x$ and fluid 2 | K |
| $\omega$ | angular speed | $s^{-1}$ |

*Subscripts*

| | |
|---|---|
| b | base of the fin |
| d | dissipated |
| e | end or tip of the fin |
| f | fin |
| h | refers to convective heat transfer |
| $i$ | index (a natural number) of considered cell; refers to input admittance |
| $i-\Delta, i+\Delta$ | point $\Delta x/2$ before or after central point $i$ of a cell |
| m | mean value of the harmonic wave |
| NSM | refers to Network Simulation Method |
| o | output |
| s | source |
| u | refers to the unfinned wall |
| w | wall |
| $x, y$ | $x, y$-direction |
| 0 | initial ($t = 0$) |
| $\gamma$ | refers to capacity |
| 1 | unfinned side of the wall (left hand side of the fin-wall assembly in Fig. 1) |
| 2 | finned side of the wall (right hand side of the fin-wall assembly in Fig. 1) |
| $\infty$ | external medium far from the surface |

Only Houghton et al. [17] have analytically studied a limited pseudo-stationary response of the fin-wall set under harmonic excitation, although their results are not applicable to a properly transitory response.

In this work we present a transient numerical solution for a fin-wall assembly under simultaneous step and harmonic excitation. The heat flux values are presented alongside several versions of performance coefficients whose validity has been discussed by Kraus [18] and Wood et al. [19]. Classical definitions have been rewritten for the characterisation of the fin-wall assembly, under the above-specified boundary conditions at the base. The adequacy of classical fin performance coefficients has been discussed for the study of fin-wall systems subject to transitory and harmonic excitations.

On the other hand, the frequency which thermal systems can be subject to offers a wide variation: from once a day (day-night cycles) up to more than 20000 rpm in some internal combustion engines. For that reason it is important to analyse the behaviour of the characteristic variables of the system in relation to the frequency of the harmonic temperature. Nevertheless a systematic study of this variation has not been performed to date.

In this paper we make use of thermal frequency response analysis. This, applied to a complex thermal transmission functions such as thermal reverse admittance, enables us to obtain the system's frequency response. The Network Simulation Method (NSM) is particularly apt to evaluate the module, phase and real and imaginary parts of those functions.

NSM is a general-purpose technique whose efficiency has been established for different non-lineal problems, both in the heat transfer domain [20] and other fields [21]. The NSM is quite capable of dealing with lineal and non-lineal problems, in a relatively easy way. The inclusion of more complex conditions than those of classical hypotheses is really simple and the assumptions of any kind of non-lineal boundary conditions, including the base excitation, may also be assumed with no special requirements.

## 2. Fin-wall assembly model

We consider the longitudinal straight fin and wall assembly shown in Fig. 1. The transversal dimensions of the fin and wall are shown and the fin thickness satisfies the $2e \ll b$ condition. The fin base is attached to the wall through perfect thermal contact. We also assume a 1-D uniform and isotropic flux through the section. No internal heat generation, constant thermal conductivity $k_{\mathrm{f}}, k_{\mathrm{w}}$ and specific heat $c_{\mathrm{f}}, c_{\mathrm{w}}$ of the fin and wall materials are assumed for simplicity. Four heat transfer coefficients exist in the set, named $h_1, h_{2\mathrm{w}} h_{2\mathrm{f}}$ and $h_{2\mathrm{e}}$. Subscripts 1 and 2 refer to the hot (left-hand side) and cold (right-hand side) fluids, respectively; subscripts w, f and e refer to wall, bulk fin and end fin surfaces, respectively. The values of the four heat transfer coefficients are assumed to be constant. Under these hypotheses the temperature at the fin base $T_{\mathrm{b}}$ is uniform and it is not known beforehand. Due to symmetry, only the section of the assembly between $y = 0$ and $y = L_y$ needs to be analysed. The mathematical model consists of the following set of equations:

$$t > 0,\ 0 < x < L_{\mathrm{w}}:$$
$$\partial j_{\mathrm{w}}/\partial x + \rho_{\mathrm{w}} c_{\mathrm{w}}(\partial T/\partial t) = 0$$
$$j_{\mathrm{w}} = k_{\mathrm{w}}(\partial T/\partial x) \tag{1}$$
$$t > 0,\ L_{\mathrm{w}} < x < L_{\mathrm{w}} + L_{\mathrm{f}}:$$
$$\partial j_{\mathrm{f}}/\partial x + \rho_{\mathrm{f}} c_{\mathrm{f}}(\partial T/\partial t) + h_{2\mathrm{f}}(P/S_{\mathrm{f}})(T - T_{2\infty}) = 0$$
$$j_{\mathrm{f}} = k_{\mathrm{f}}(\partial T/\partial x) \tag{2}$$
$$t > 0,\ x = 0: \quad k_{\mathrm{w}} \partial T/\partial x = h_1(T - T_{1\infty}) \tag{3}$$
$$t > 0,\ x = L_{\mathrm{w}}: \quad T_{\mathrm{w}} = T_{\mathrm{f}} \tag{4}$$
$$t > 0,\ x = L_{\mathrm{w}}: \quad S_{\mathrm{w}} k_{\mathrm{w}} \partial T/\partial x = S_{\mathrm{f}} k_{\mathrm{f}} \partial T/\partial x + (S_{\mathrm{w}} - S_{\mathrm{f}}) h_{2\mathrm{w}}(T - T_{2\infty}) \tag{5}$$
$$t > 0,\ x = L_{\mathrm{w}} + L_{\mathrm{f}}: \quad k_{\mathrm{f}} \partial T/\partial x = h_{2\mathrm{e}}(T - T_{2\infty}) \tag{6}$$
$$t = 0,\ 0 < x < L_{\mathrm{w}} + L_{\mathrm{f}}: \quad T = T_0 \tag{7}$$
$$t > 0: \quad T_{1\infty} = T_{\mathrm{m}}\big[1 + A\cos(\omega t)\big] \tag{8}$$
$$t > 0: \quad T_{2\infty} = 0 \tag{9}$$

where the temperature $T = T(x, t)$ is the dependent variable, and position, $x$, and time, $t$, the independent variables. $j$ is the heat flux density ($\mathrm{W \cdot m^{-2}}$), $\rho$ the density, $P$ the external perimeter of the fin section ($P = 2e + b$), $S_{\mathrm{w}}$ the section of the wall ($S_{\mathrm{w}} = bL_y$), $S_{\mathrm{f}}$ the section of the fin ($S_{\mathrm{f}} = eb$), and $T_0$ a constant value. Eqs. (1) and (2) are the local heat conduction equations for the wall and fin, respectively, being the fluxes $j_{\mathrm{w}}$ and $j_{\mathrm{f}}$ defined by the Fourier equation. Eqs. (3), (4), (5) and (6) are associated to the boundary conditions at $x = 0$, $x = L_{\mathrm{w}}$ and $x = L_{\mathrm{w}} + L_{\mathrm{f}}$, respectively. Eq. (7) is the initial condition, a constant value has been assumed for simplicity. Finally, Eq. (8) corresponds to a step-harmonic excitation source, where $T_{\mathrm{m}}$ is the mean (step) value of the harmonic temperature, $A$ is a non-dimensional constant and $\omega = 2\pi f$, with $f$ being the frequency of the excitation (Fig. 1).

## 3. The network simulation method

The numerical technique employed to solve the problem is the Network Simulation Method. As is well known, the mathematics behind the dynamic behaviour of systems from different disciplines of physics have much in common. Thermodynamic systems in particular, can be studied using electrical analogy. This methodology was formalized in the early seventies by means of the so-called network thermodynamics [22], which permits coupled flows and driving forces to be analized in terms of linear graphs, as electrical networks. In this sense, NSM takes advantage of the similarities in the mathematical structure underlying different phenomena with balance and constitutive equations of the same type. Such equations fix the topology (the connection modes of the circuit branches) and the geometry (the circuit elements: resistors, capacitors, inductors, sources, etc.) of the network model, thus allowing us to establish a formal similitude between the transport equations and the electrical networks. This formal similitude is used by the NSM to obtain information about the behaviour of the system considered.

A set of ordinary differential equations are obtained by spatial discretization of the mathematical model, generally defined by differential equations; namely, (i) partial differential conduction heat equation, (ii) boundary equation, (iii) initial condition, and (iv) specific differential equations referred to the medium or to the boundary conditions. Time $t$ is maintained as a continuous independent variable. To this end, the wall and the fin are divided into $N_{\mathrm{w}}$ and $N_{\mathrm{f}}$ volume elements or cells of length $\Delta x_{\mathrm{w}} = L_{\mathrm{w}}/N_{\mathrm{w}}$ and $\Delta x_{\mathrm{f}} = L_{\mathrm{f}}/N_{\mathrm{f}}$. From these last equations, a network model for an elementary cell or control volume of the medium is designed

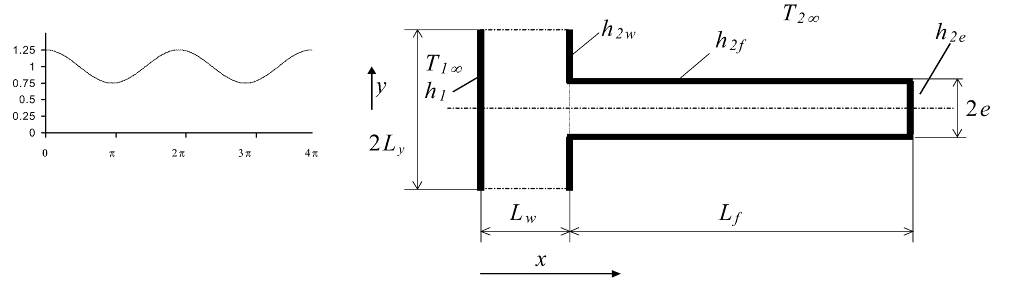


Fig. 1. Transversal section of the fin-wall assembly.

associating different electrical ports to every term that integrates the differential conduction equations. By connecting in series ($N$) of these elemental networks, the model for the whole medium is obtained; boundary conditions are implemented with additional electrical devices connected to the boundaries. Using NSM in non-lineal 1-D problems, such as temperature dependent thermal characteristics or moving boundary problems, errors are below 0.5% for a number of volume elements $N \geqslant 50$ [23].

From Eqs. (1) and (2), using (3), the following ordinary differential equations are obtained,

$$J_{i-\Delta} - J_{i+\Delta} = \rho c S_x \Delta x \frac{\partial T}{\partial t} \tag{10}$$

$$J_{i\pm\Delta} = \pm k_{i\pm\Delta} S_x \frac{(T_i - T_{i\pm\Delta})}{\Delta x/2} \tag{11}$$

$$\begin{aligned} &J_{h2\mathrm{w}} = h_{2\mathrm{w}}(S_\mathrm{w} - S_\mathrm{f})(T_{x=L_\mathrm{w}} - T_{2\infty}) \quad \text{(wall)} \\ &J_{h2\mathrm{f}} = h_{2\mathrm{f}} P \Delta x (T_i - T_{2\infty}) \quad \text{(fin)} \end{aligned} \tag{12}$$

$$J_{i\gamma} = \rho c S_x \Delta x \frac{\partial T}{\partial t} \tag{13}$$

$T_i$, $T_{i-\Delta}$ and $T_{i+\Delta}$ are the temperatures at the centre and ends of the cell, respectively (Fig. 2(a)). The convection flux at each cell is implemented by a resistance, which establishes the relationship between heat flow and excess. The network model for the fin-wall system is showed in Fig. 2(b).

Heat conservation is inherent in the network because of Kirchhoff's conservation law for electric currents, so that no additional requirements are needed. The same applies to the uniqueness of the temperature fields, which are satisfied by the Kirchhoff's voltage law.

The values for the lineal elements, resistors and capacitors are:

$$\begin{aligned} R_{i\pm\Delta,\mathrm{w}} &= \frac{\Delta x_\mathrm{w}}{2k_{i\pm\Delta,\mathrm{w}} S_\mathrm{w}} = \frac{\Delta x_\mathrm{w}}{2k_{i\pm\Delta,\mathrm{w}} b L_y} \\ R_{i\pm\Delta,\mathrm{f}} &= \frac{\Delta x_\mathrm{f}}{2k_{i\pm\Delta,\mathrm{f}} S_\mathrm{f}} = \frac{\Delta x_\mathrm{f}}{2k_\mathrm{f} b e} \end{aligned} \tag{14}$$

$$\begin{aligned} R_{\mathrm{h1}} &= \frac{1}{h_1 S_\mathrm{w}} = \frac{1}{h_1 b L_y} \\ R_{\mathrm{h2w}} &= \frac{1}{h_{x=L_\mathrm{w}}(S_\mathrm{w} - S_\mathrm{f})} = \frac{1}{h_{2\mathrm{w}} b (L_y - e)} \end{aligned} \tag{15}$$

$$\begin{aligned} R_{\mathrm{h2f}} &= \frac{1}{h_{2\mathrm{f}} P \Delta x_\mathrm{f}} = \frac{1}{h_{2\mathrm{f}}(2e + b)\Delta x_\mathrm{f}} \\ R_{\mathrm{he}} &= \frac{1}{h_{2\mathrm{e}} S_\mathrm{f}} = \frac{1}{h_{2\mathrm{e}} b e} \end{aligned} \tag{16}$$

$$C_{i\mathrm{w}} = \rho_\mathrm{w} \cdot c_\mathrm{w} S_\mathrm{w} \Delta x_\mathrm{w} = \rho_\mathrm{w} \cdot c_\mathrm{w} b L_y \Delta x_\mathrm{w} \tag{17}$$

$$C_{i\mathrm{f}} = \rho_\mathrm{f} \cdot c_\mathrm{f} S_\mathrm{f} \Delta x_\mathrm{f} = \rho_\mathrm{f} \cdot c_\mathrm{f} b e \Delta x_\mathrm{f} \tag{18}$$

Once we have obtained the general network model, its simulation provides the temporal evolution and stationary values for the heat flux and temperature variables, in any section or any point of the cell, respectively. Very few programming language sentences are necessary to make the program files run on PSpice software, and those that are necessary are quite straightforward. Once the network model for a cell is programmed, PSpice recognises it as a subcircuit that may be implemented as many times as required (in order to simplify the program). The interactive design warns the programmer about possible errors and depicts the correct way of operation.

Based on this tool, a network model (Fig. 2(b)) is designed from the mathematical model above, the network equations being formally equivalent to the ordinary differential equations obtained by discretising the partial differential equations of the mathematical model. Time is maintained as a continuous variable. The NSM application is very illustrative of general transport processes, because of the direct visualisation of the transport variable as an electric current

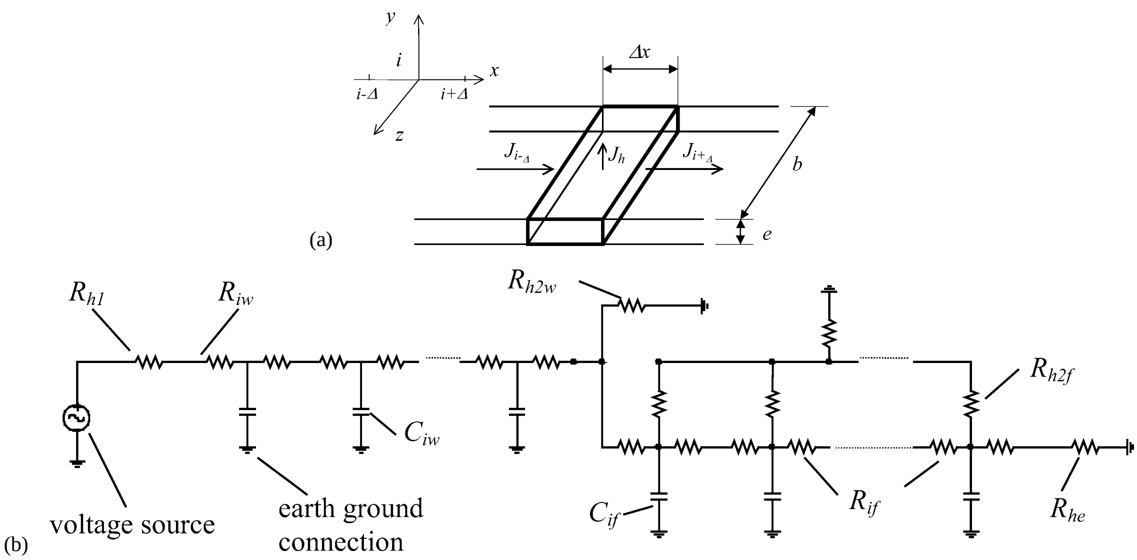


Fig. 2. (a) Volume element, and (b) Network model of the fin-wall assembly.

and its inherent conservation law. Once the network model is designed, its simulation is carried out through an adequate circuit resolution software; PSpice® is the software selected for this study [24].

## 4. Transient step-harmonic excitation responses

Application is made to an aluminium fin-wall of the following geometrical and thermal characteristics: $k_{\mathrm{f}} = k_{\mathrm{w}} = 229\ \mathrm{W{\cdot}m^{-1}{\cdot}K^{-1}}$; diffusivity $\alpha_{\mathrm{f}} = \alpha_{\mathrm{w}} = k/(\rho c) = 9.733\mathrm{E{-}5}\ \mathrm{m^2{\cdot}s^{-1}}$; $L_y = 2\mathrm{E{-}3}$ m; $L_{\mathrm{f}} = 1 \div 8\mathrm{E{-}2}$ m; $L_{\mathrm{w}} = 2 \div 8\mathrm{E{-}3}$ m; $e = 8 \div 16\mathrm{E{-}4}$ m; $h_1 = 1\mathrm{E{-}2} \div 1\mathrm{E{-}4}\ \mathrm{W{\cdot}m^{-2}{\cdot}K^{-1}}$; $h_{2\mathrm{w}} = h_{2\mathrm{f}} = h_{2\mathrm{e}} = 10 \div 1\mathrm{E{-}3}\ \mathrm{W{\cdot}m^{-2}{\cdot}K^{-1}}$; $f = 0.0001 \div 100\ \mathrm{s^{-1}}$. The frequency range of the study practically covers the whole range to which ordinary thermal systems are subject. Values of $T_{\mathrm{m}} = 1$, $A = 0.25$ and $T_0 = 0$ have been taken for the simulation. If we define temperature excess or simply excess $\theta = T - T_{2\infty}$, then all the results are related to a 1 K mean temperature excess. Numerical results are presented in dimensionless form, with $M = (2h_{2\mathrm{f}}L_{\mathrm{f}}^2/2ek_{\mathrm{f}})^{1/2}$, $B = \omega L_{\mathrm{f}}^2/\alpha$ and $Fo = t\alpha/L_{\mathrm{f}}^2$ the classical dimensionless numbers used in this kind of fin problem. According to the above domains of selected thermal and geometrical parameters, the ranges of values of the dimensionless numbers are $M = 0.15 \div 1.48$ and $B = 2.58\mathrm{E{-}03} \div 2.58\mathrm{E{-}03}$. The number of cells in the network model is 60; 20 corresponding to the wall, due to its thickness, and 40 to the fin. Computing time for this problem in all the simulated cases was less than 1 s in a Pentium III PC.

For comparison purposes, analytical and numerical fin temperatures were evaluated during the pseudo-stationary state, which is defined as the state where the wave repeats indefinitely after the transient period. Fig. 3 compares one cycle of numerical temperatures, $T_{\mathrm{NSM}}$, results in the middle of the fin ($x = L_{\mathrm{w}} + L_{\mathrm{f}}/2$) and at its base ($x = L_{\mathrm{w}}$), with those analytically obtained by Houghton et al. [17] for the pseudo-stationary case, in terms of the error defined as $e(\%) = 100 \cdot (T_{\mathrm{NSM}} - T)/T$. Error fit curves are depicted in the Fig. 3, the wave form being due to the oscillation of the denominator in relative error expression; the absolute error $\cdot\ |T_{\mathrm{NSM}} - T|$ remains practically the same throughout the cycle. For both places, the NSM numerical results are very close to the analytical results and errors are within an acceptable range in practical application. These results confirm that the discretisation carried out in the fin-wall assembly is quite acceptable.

In the present work we focus on a study of the transient time before the pseudo-cyclic steady state is reached. This transient lapse has been computed as the time needed for the mean value of the signal (bias point) to reach 99% of its final value. Fig. 4 shows this transient response for a temperature excess $\theta$ and heat rate $J = jS$ for step-harmonic excitation; delay and damping phenomena may be observed in both variables. Fig. 5 shows the temperature variation at the middle of the fin for different values of $B$; which oscillates around the mean value, which is just $B = 0$ or non-harmonic excitation. The initial transient time before the pseudo-stationary period is not affected by the values of $B$. As a consequence, a fin-wall system under step-harmonic excitation and the hypothesis established in Section 2, behaves as a system subject to both step and harmonic excitation and the transient time is not influenced by the

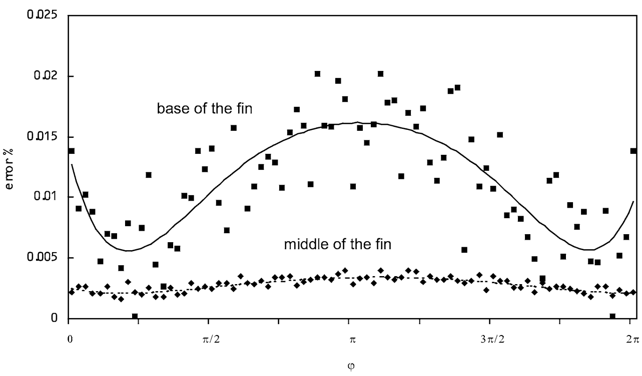


Fig. 3. Temperature error in a fin-wall assembly with step-harmonic excitation. Comparison with Houghton et al. [17]. $x = L_{\mathrm{w}}$ (base) and $x = L_{\mathrm{w}} + L_{\mathrm{f}}/2$ (middle).

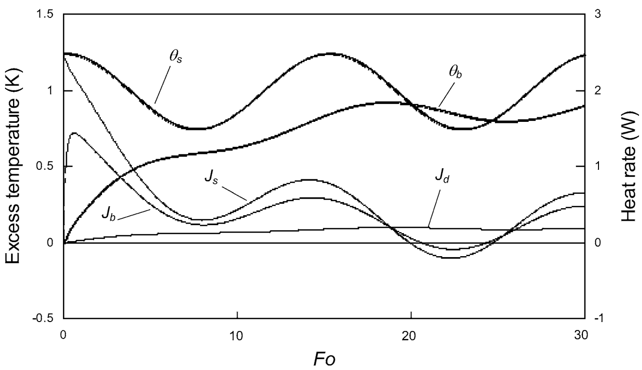


Fig. 4. Transient evolution of heat rate and temperature in a fin-wall assembly with step-harmonic excitation. $M = 0.148$, $B = 20.05$, $\theta_{\mathrm{m}} = T_{\mathrm{m}} - T_{2\infty} = 1$ K and $A = 0.25$.

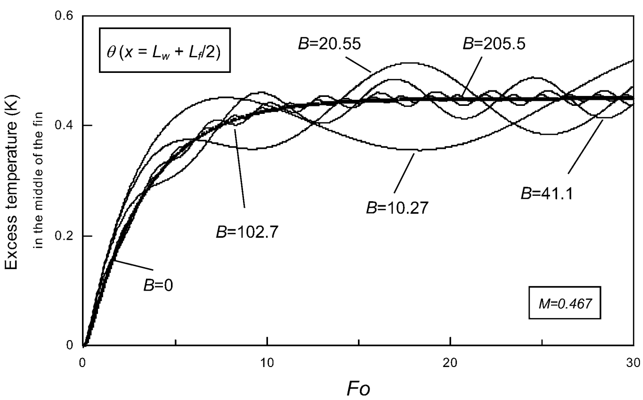


Fig. 5. Transient temperature in the middle of the fin ($x = L_{\mathrm{w}} + L_{\mathrm{f}}/2$) under step-harmonic excitation for different $B$ values.

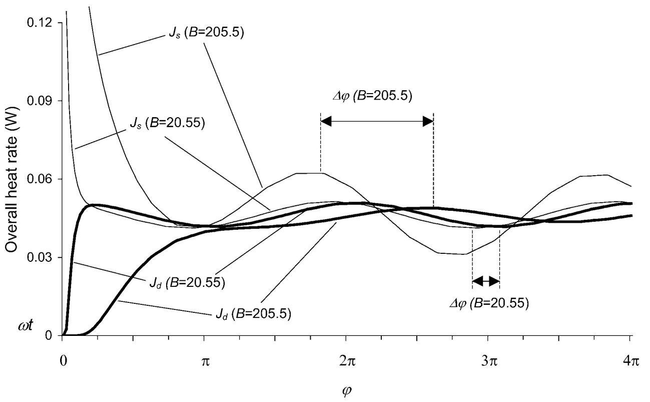


Fig. 6. Transient overall heat source rate $J_s$ and heat dissipated rate $J_d$, as a function of the angle, under step-harmonic excitation for different $B$ values.

oscillatory component. The amplitude of the wave gradually grows until it reaches the cyclic steady-state value. On the other hand, as some authors predict [1–3] for the isolated fin, temperature and heat flux amplitude values in the fin-wall assembly fall substantially as frequency increases. The thermal frequency response analysis, which we introduce in the next section, allows us to generalise this assertion.

The total heat dissipated by the fin-wall assembly subjected to a step-harmonic excitation $J_d$, which is the integrated heat rate over the whole surface washed by fluid 2 and the heat flow from source $J_s$, which is the heat rate across surface 1, are shown in Fig. 6 for $B = 20.55$ and 205.5. In time-dependent processes the heat fluxes are different.

For these numerical values, the existing delay between fluxes $J_s$ and $J_d$, $|\Delta\varphi| = |\varphi_s - \varphi_d|$, increases with $B$. From Fig. 6, for $B = 20.55 |\Delta\varphi| = 0.655$ rad and for $B = 205.5$ $|\Delta\varphi| = 2.01$ rad. On the other hand, the delay between source fluxes for different frequencies is $|\Delta\varphi_s| = |\varphi_s(B = 20.55) - \varphi_s(B = 205.5)| = 0.315$ rad and between dissipated fluxes is $|\Delta\varphi_d| = |\varphi_d(B = 20.55) - \varphi_d(B = 205.5)| = 1.03$ rad. When $B$ grows the amplitude of $J_s$ grows accordingly, while the amplitude of $J_d$ decreases slightly. This fact can be explained by the network model, since the input impedance of the network decreases with frequency due to cumulative thermal effects ($J_s$ grows). So, when frequency grows the system offers less resistance to the heat transfer and the heat does not cross the fin-wall towards the surrounding medium ($J_d$ decreases).

On the other hand, the wave peaks of $J_s$ move towards the left-hand side of the figure, i.e., the delay in $J_s$ with respect to the input signal (excess temperature) decreases when the frequency grows, while the wave peaks of $J_d$ move towards the right-hand side, i.e., the delay in $J_d$ grows as the frequency increases. Again the explanation of this effect can be found in the network model: as frequency increases, the material has greater difficulty in following the excitation signal. Frequency response analysis allows this assertion to be generalised (see Section 6).

With respect to the fin-wall transient lapse, we have found that it is not possible to establish a direct relationship

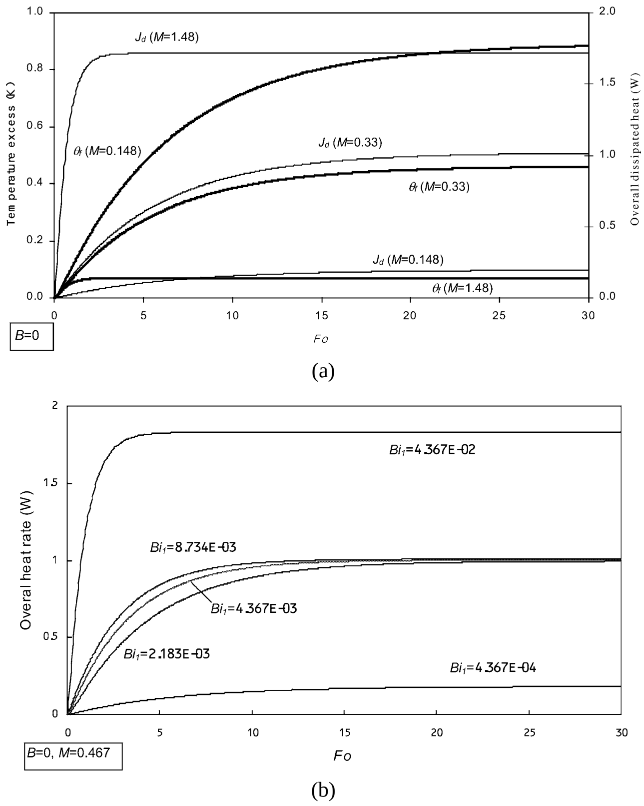


Fig. 7. Transient response in a fin-wall assembly submitted to a step excitation ($B = 0$). (a) Excess temperature $\theta_f$ in the middle of the fin and overall dissipated heat rate $J_d$ dependent of $M$-parameter, and (b) Overall dissipated heat rate $J_d$ in dependence of $Bi_1$.

between the transient times of a fin-wall, an isolated fin and a naked wall. In conclusion, it is necessary to evaluate the complete assembly to study its transient behaviour.

Initial transient time of the fin-wall system under a step (not oscillatory) excitation as a function of the parameter $M$ is shown in Fig. 7(a), where a similar behaviour of temperatures and fluxes may be observed. It can also be appreciated that the transient time of temperature and heat rate decreases when $M$ increases.

Fig. 7(b) refers to the same excitation for identical fins ($M = 0.467$) and different modified Biot numbers ($Bi_1 = h_1 L_y^2 / k_w L_w$), i.e., different wall thickness and/or heat transfer coefficient $h_1$. The central curves of this figure correspond to the variation of $L_w$. The smaller the wall thickness the shorter the transient time. On the other hand, transient time grows considerably if either $h_1$ or $Bi_1$ decrease (upper, set of medium and lower curves). The fin-wall assembly subject to $h_2$ variation has a similar behaviour, but in a considerable less marked way. This is due to the fact that the temperature in the fin decreases noticeably in relation to the heat source (the hot fluid) and then the convective term is much less in the cold side than in the hot side of the assembly.

## 5. Thermal reverse admittance

NSM makes possible the direct evaluation of some transmission functions that try to quantify the ability of the fin-wall system for heat dissipation, both in stationary and in transient regimes.

We have first studied the efficiency $\eta$ (more used than the effectiveness by the fin designers). The fin efficiency in an isolated fin is defined as the ratio between the actual heat flow rate dissipated by the fin $J_{\rm d}$ and that which would be dissipated if the whole fin were at the base temperature $J_{\rm d}(\theta_{\rm b})$:

$$\eta = \frac{J_{\rm d}}{J_{\rm d}(\theta_{\rm b})} = \frac{J_{\rm d}}{h_{2\rm f} S_{\rm f}^* \theta_{\rm b}} \tag{19}$$

where $J_{\rm d}$ is the overall heat rate dissipated by the fin, $S_{\rm f}^*$ the external surface of the fin, and $\theta_{\rm b}$ the base temperature excess. For stationary systems $\theta_{\rm b}$ is constant, and the dissipated heat rate $J_{\rm d}$ coincides with the heat rate through the fin base $J_{\rm b}$. In this case there is no difference between $\eta$ and the efficiency $\eta_{\rm b}$, associated with the instantaneous heat through the base fin:

$$\eta_{\rm b} = \frac{J_{\rm b}}{J_{\rm d}(\theta_{\rm b})} = \frac{J_{\rm b}}{h_{2\rm f} S_{\rm f}^* \theta_{\rm b}} \tag{20}$$

When $\theta_{\rm b}$ and, as a consequence, $J$ are time-dependent $\eta \neq \eta_{\rm b}$ and the efficiency ought to be defined by instantaneous fluxes. By using NSM instantaneous efficiencies $\eta$ and $\eta_{\rm b}$ of a fin built in a step-harmonically-excited fin-wall system have been computed. Fig. 8 shows the differences between $\eta$ and $\eta_{\rm b}$. During the initial transient time they are very different; they oscillate around the response to step excitation with the same frequency as the exciting source (similar behaviour to an isolated fin under harmonic excitation, as Yang [1] predicted). At the stationary time their values converge to that of the step excitation. A significance difference in the amplitude of $\eta$ and $\eta_{\rm b}$ is also observed. If we consider that for design tasks the important flux is the dissipated heat rate, we can conclude that there exists a fair superiority of $\eta$ over $\eta_{\rm b}$.

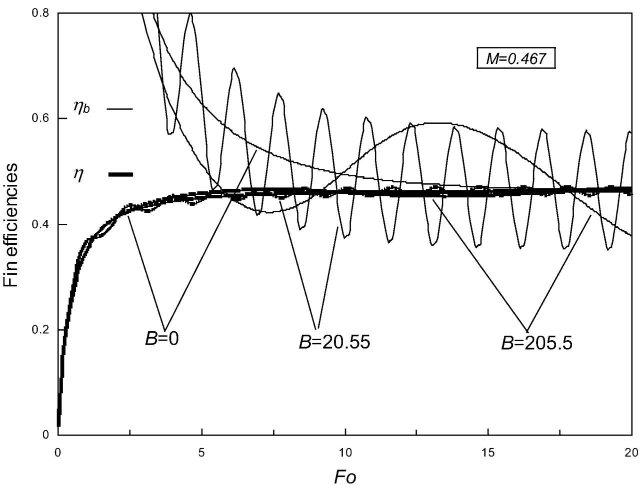


Fig. 8. Fin efficiencies referred to the heat rate dissipated by the fin ($\eta$) or to the base heat rate ($\eta_{\rm b}$), for different frequencies.

The augmentation coefficient Aug, proposed by Heggs et al. [10], seems to have some advantages over other performance indicators of fin-wall systems in stationary processes (Wood et al. [19]). Aug is a measurement of the exceeding dissipated heat in a wall when the fin is added. It is obviously necessary that the thermal gradient and/or boundary conditions on the surfaces of the wall are the same in order to compare the heat fluxes. In this work we propose its generalisation to time-dependent processes. If we call $J_{\rm d,u}$ the heat rate dissipated by the unfinned wall

$$\mathrm{Aug} = \frac{J_{\rm d}}{J_{\rm d,u}} = \frac{\text{Instantaneous heat flow through the fin} - \text{wall assembly}}{\text{Instantaneous heat flow through the plain wall}} \tag{21}$$

Fig. 9(a) shows the Aug factor for different frequencies; Aug is a harmonic function too. Aug oscillates during the transitory around the value associated to the step excitation, and its amplitude decreases with higher frequencies. The influence of the parameter $M$, which only contains fin information, in the Aug factor is represented in Fig. 9(b). The curve for $M = 0.33$ is initially below that of $M = 0.467$,

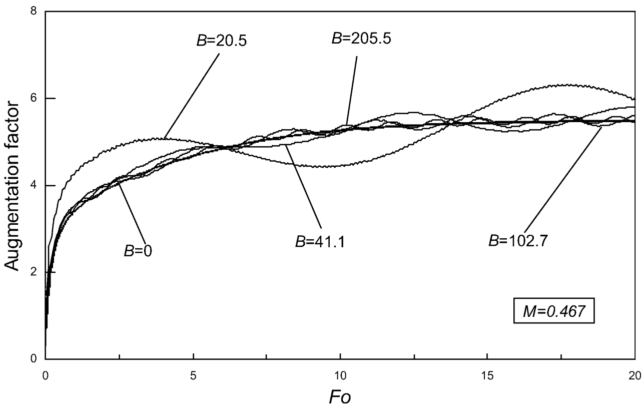


(a)

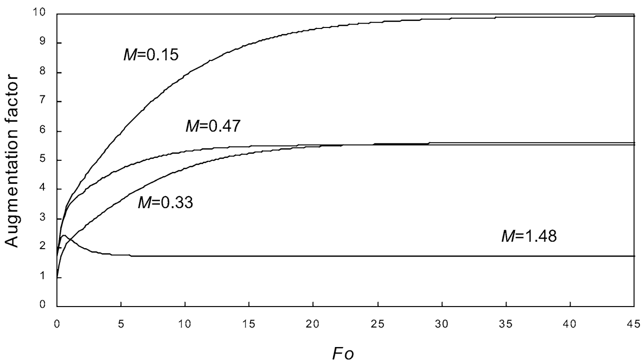


(b)

Fig. 9. Augmentation factor during transient response of a fin-wall system. (a) For different $B$-parameter (i.e., frequencies), and (b) For different $M$-coefficients and constant wall thickness under step excitation.

but as the stationary time is reached, it gets above it. Besides, both curves are below the one corresponding to $M = 1.478$ in the beginning of the transition. This result questions the use of parameter $M$ in the study of fin-wall systems transient time.

Nevertheless, a thermal characterisation of the fin-wall assembly can be done in a more general way with using thermal transmission functions, which relate the stimulus and the thermal response of the system. Thus the fin-wall system may be considered as a two-entry system, where the input is the excess temperature $\theta$ and the output is the dissipated heat rate. The relationship between input and output is ruled by a set of equations, which constitutes the mathematical model or its equivalent network model. Therefore, from the perspective of the thermal transmission functions, the network model has got an electric admittance, which exactly reproduces the thermal admission of the fin-wall system.

We define the *thermal reverse transfer admittance*, or simply *thermal reverse admittance* as

$$Y_r = \frac{J_d}{\theta_s} \tag{22}$$

where $\theta_s$ is the excess in the input section of the system, i.e. the source. Once the input signal is known, $Y_r$ may be calculated with the determination of its amplitude and phase, just as the dependence of such parameters with the frequency of input signal. NSM is especially useful to study complex thermal transmission functions, such as admittance, directly evaluating module, phase, and real and imaginary components. The implementation of the network model in an electrical circuit simulation program such as PSpice [24] enables us to obtain the thermal admittance of the system. For this purpose PSpice uses the following procedure:

(a) to determine the steady-state conditions of the system (the bias point), the program solves the transport equations together with the initial and boundary conditions by using only the independent source component;
(b) the transport equations and the boundary conditions are linearized about the bias point calculated above;
(c) finally, the sinusoidal response signal of the system in the steady-state is determined.

Fig. 10(a) shows the variation of module, phase, real and imaginary parts of the thermal reverse admittance in a fin-wall assembly where $M = 0.467$ and the non-dimensional angular speed $B$ varies between 2.58E–03 and 2.58E03. The module and phase have an evident dependence on frequency. At a low $B$ the amplitude is relatively high, then it quickly decreases and at a greater $B$ the module is zero in practice. It seems that at low frequencies the material could reflect the excitation, but not at higher frequencies. The phase, always negative, decreases as the $B$-parameter grows. This behaviour implies that the instantaneous fluxes have opposite directions in a certain frequency range. This means that the heat flow can simultaneously enter or get out of the two ports (excited and dissipation surfaces). This seeming incongruity appears when the real part of the output wave has negative sign. In the considered system this fact occurs in a range of frequencies for which the amplitude is still very low.

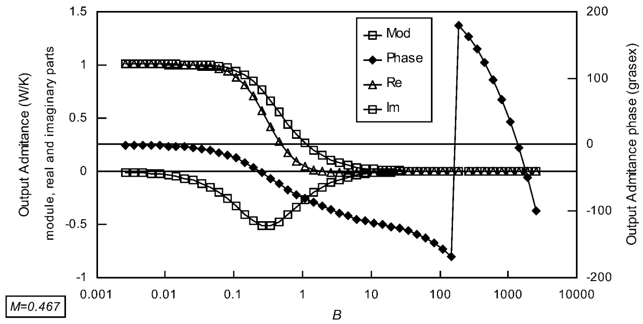


(a)

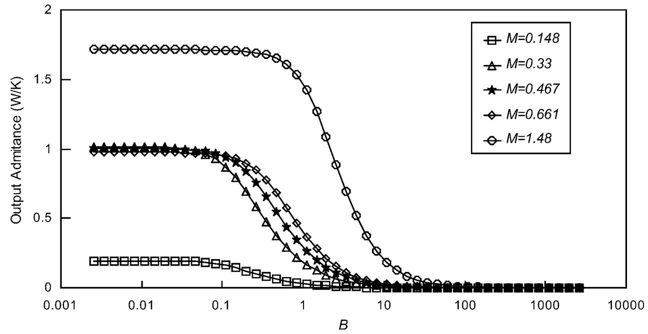


(b)

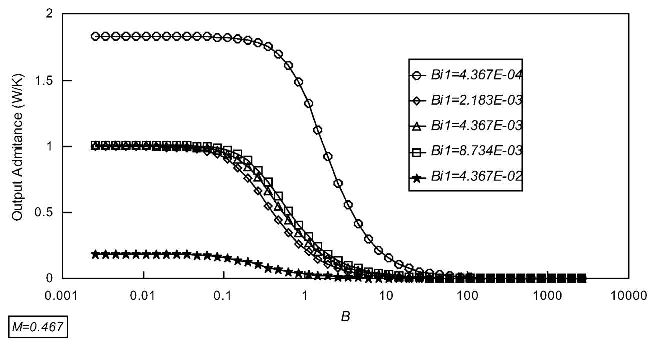


(c)

Fig. 10. Thermal reverse admittance frequency response, $Y_r$, of a fin-wall assembly (as a function of non-dimensional frequency $B$). (a) Module, phase, real and imaginary parts; (b) For different $M$-parameters and the same geometry, and (c) As a function of $Bi_1$ parameter and $M = 0.467$.

Fig. 10(b) represents module variation of the fin-wall system thermal reverse admittance for different $M$-parameters. In all cases a rather abrupt fall in amplitude is observed and, into the range of two decades of frequency, the module practically vanishes. The damping of the wave occurs at lower frequencies, as $M$ becomes smaller. In metallic thermal systems this damping occurs at relatively low frequencies. Thus, in the aluminium fin the amplitude is quite negligible at a frequency of 1 Hz for any value of $M$. Fig. 10(c) shows the frequency response of the fin-wall system with

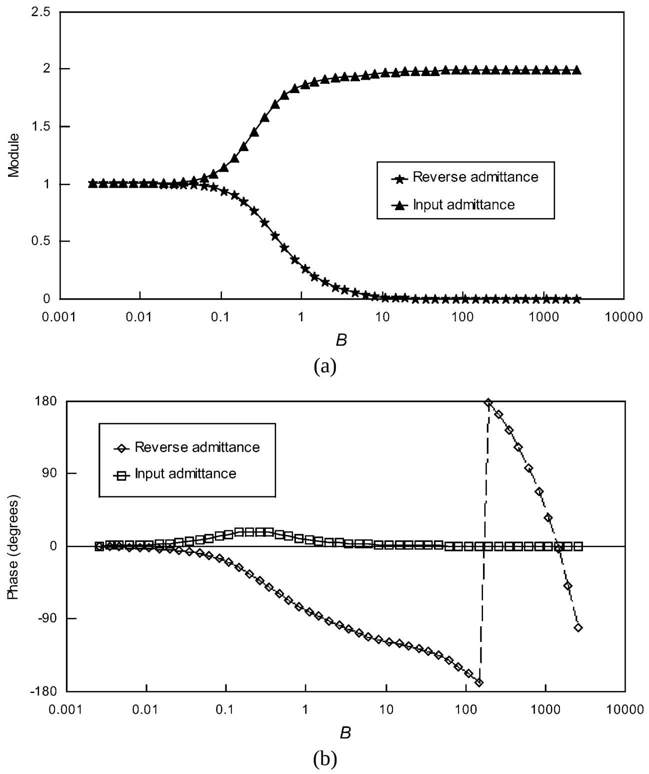


Fig. 11. Frequency response analysis of input admittance, $Y_i$, and reverse admittance, $Y_r$. (a) Module; (b) Phase.

$Bi_1$, which corresponds to the variation of wall thickness $L_w$ (the central set of curves) and $h_1$ (upper, mid and lower curves). We detect a much bigger response sensitivity to the variation of the latter.

Fig. 11 depicts the frequency response analysis of the input admittance compared with the reverse admittance. Input admittance, $Y_i$, a fin performance parameter first introduced by Kraus [18] and now used generally, relates $J_s$ and $\theta_s$:

$$Y_i = \frac{J_s}{\theta_s} \tag{23}$$

At low frequencies both $Y_i$ and $Y_r$ parameters are identical because the thermal inertia of the assembly is negligible. However as frequency increases both the module and phase of $Y_i$ and $Y_r$ are quite different. While $Y_r$ tends to zero (as does $J_d$), $Y_i$ increases to a limit value, i.e., the amplitude of $J_s$ increases substantially at high values of frequency. This means that the oscillation peaks are much greater when the frequency is high. This is in concordance with the facts discussed in Section 4, where it was said that with increasing frequency the amplitude of $J_s$ grows while the amplitude of $J_d$ diminishes. With respect to the phase delay, it is noticeable that the $Y_i$ phase shows a maximum at medium frequencies and tends to zero at low and high frequencies.

## 6. Conclusions

This paper presents a study of a fin-wall assembly under step-harmonic excitation conditions to obtain the transient and stationary responses. To this end, a distributed 1-D network model based on the Network Simulation Method is used. The transient response of the fin-wall system, which must be evaluated as an assembly, oscillates around the transient response resulting from step (non-harmonic) excitation. The amplitude of the harmonic component gradually grows during the transient time until it reaches that of the cyclic pseudo-steady state. This means that to compute the transient time of a fin-wall system subject to step-harmonic excitation, due to the lineality, only the transient time of the step excitation needs to be calculated. Moreover, the transient time before the pseudo-steady state, which decreases as heat transfer coefficient grows or as the wall thickness decreases, does not depend on the frequency of the excitation wave.

The influence of the characteristic parameter $M$ in the fin-wall response is shown, not to represent adequately the behaviour of the assembly under this kind of excitation. Also, the influence of the dimensionless frequency, $B$, on the source and dissipated fluxes is studied, determining the module and phase of these signals, and the phase differences between them and the excitation signal.

The inconsistencies of the classical performance coefficient efficiency are shown and a new coefficient, the thermal reverse admittance, is proposed to characterise adequately the fin-wall assembly. Thermal frequency response analysis of the system has been carried out using this parameter. Module and phase versus frequency have been depicted to permit direct calculation of the harmonic component of the dissipated flux. Finally, the proposed parameter may easily be obtained by means of the network model and NSM.

## References

[1] J.W. Yang, Periodic heat transfer in straight fins, J. Heat Trans. 94 (1972) 310–314.
[2] A. Aziz, Periodic heat transfer in annular fins, J. Heat Trans. 97 (1975) 302–303.
[3] N.V. Suryanarayana, Transient response of straight fins, J. Heat Trans. 97 (1975) 417–423.
[4] N.V. Suryanarayana, Transient response of straight fins. Part II, J. Heat Trans. 98 (1976) 324–326.
[5] H.S. Chu, C.I. Weng, C.K. Cheng, Transient response of a composite straight fin, J. Heat Trans. 105 (1983) 307–311.
[6] S.S. Wu, C.L. Shiu, W.J. Wu, Analysis on transient heat transfer in annular fins of various shapes with their bases subjected to a heat flux varying as a sinusoidal time function, Comput. Struct. 61 (1996) 725–734.
[7] Xiangxiang Yang, Hongzhou He, Periodic heat transfer in the fins with variable thermal parameters, Appl. Math. Mech. (English ed.) 17 (1996) 169–180.
[8] K.D. Papadopoulos, A.G. Guzman-Garcia, R.V. Bailley, The response of straight an circular fins to fluids temperature changes, Internat. J. Heat Mass Trans. 17 (1990) 587–595.

[9] N.V. Suryanarayana, Two-dimensional effects on heat transfer rates from an array of straight fins, J. Heat Trans. 99 (1977) 129–132.
[10] P.J. Heggs, P.R. Stones, Improved design methods for finned tube heat exchanger, Trans. Ichem. Engrg. 58 (1980) 147–154.
[11] M. Manzoor, D.B. Ingham, P.J. Heggs, The one-dimensional analysis of fin assembly heat transfer, J. Heat Trans. 105 (1983) 646–651.
[12] M. Manzoor, D.B. Ingham, P.J. Heggs, Improved formulations for the analysis of convecting and radiating finned surfaces, AIAA J. 21 (1982) 120–126.
[13] L.J. Huang, R.K. Shah, Assessment of calculation methods for efficiency of straight fins of rectangular profile, ASME-HTD Adv. Heat Exchanger Design, Radiation and Combustion 182 (1991) 19–30.
[14] P.C.S. Jucá, A.T. Prata, Two-dimensional fins attached to a thick wall-effect of non-uniform root temperature, Internat. J. Heat Mass Trans. 36 (1993) 233–236.
[15] A.S. Wood, G.E. Tupholme, M.I.H. Bhatti, P.J. Heggs, Steady-state heat transfer through extended plane surfaces, Internat. Commun. Heat Mass Trans. 22 (1995) 199–209.
[16] L.C. Thomas, Heat transfer in fin assemblies: Significance of two-dimensional effects—a reexamination of the issue, J. Heat Trans. 121 (1999) 748–752.
[17] J.M. Houghton, D.B. Ingham, P.J. Heggs, The one-dimensional analysis of oscillatory heat transfer in a fin assembly, J. Heat Trans. 114 (1992) 548–552.
[18] A.D. Kraus, Analysis of extended surface, J. Heat Trans. 110 (1988) 1071–1081.
[19] A.S. Wood, G.E. Tupholme, M.I.H. Bhatti, P.J. Heggs, Performance indicators for steady-state heat transfer through fin assemblies, J. Heat Trans. 118 (1996) 310–316.
[20] C.F. González-Fernández, F. Alhama, M. Alarcón, J.F. López-Sánchez, Digital simulation of transient heat conduction with polynomial variable thermal conductivity and specific heat, Comput. Phys. Commun. 111 (1998) 53–58.
[21] J. Horno, M.T. García Hernández, C.F. González-Fernández, Digital simulation of electrochemical processes by network approach, J. Electroanal. Chem. 352 (1993) 83–97.
[22] L. Peusner, The principles of network thermodynamics: Theory and biophysical applications (Reprint of 1971 Thesis), Entropy, Lincoln, Massachusetts, 1987.
[23] F. Alhama, Study of transient thermal responses in non-lineal heat conduction processes by the Network Simulation Method, Ph.D. Thesis, University of Murcia, Spain, 1999.
[24] PSpice, 8.0 Version: Microsim Corporation, 20 Fairbanks, Irvine, California 92718, 1994.